


ARTICLE

A drug-disease model for predicting survival in an Ebola outbreak

Masood Khaksar Toroghi¹ | Nidal Al-Huniti¹ | John D. Davis¹  |
A. Thomas DiCioccio¹ | Ronda Rippley^{2,†} | Alina Baum¹ | Christos A. Kyratsous¹ |
Sumathi Sivapalasingam^{2,‡} | Joel Kantrowitz¹ | Mohamed A. Kamal¹

¹Regeneron Pharmaceuticals, Inc.,
Tarrytown, New York, USA

²Formerly of Regeneron
Pharmaceuticals, Inc., Tarrytown,
New York, USA

Correspondence

Masood Khaksar Toroghi, Regeneron
Pharmaceuticals, Inc., 777 Old Saw Mill
River Road, Tarrytown, NY 10591, USA.
Email: masood.khaksar@regeneron.com

Funding information

Regeneron Pharmaceuticals;
Biomedical Advanced Research and
Development Authority; US Army
Medical Research Institute of Infectious
Diseases

Abstract

REGN-EB3 (Inmazeb) is a cocktail of three human monoclonal antibodies approved for treatment of Ebola infection. This paper describes development of a mathematical model linking REGN-EB3's inhibition of Ebola virus to survival in a non-human primate (NHP) model, and translational scaling to predict survival in humans. Pharmacokinetic/pharmacodynamic data from single- and multiple-dose REGN-EB3 studies in infected rhesus macaques were incorporated. Using discrete indirect response models, the antiviral mechanism of action was used as a forcing function to drive the reversal of key Ebola disease hallmarks over time, for example, liver and kidney damage (elevated alanine [ALT] and aspartate aminotransferases [AST], blood urea nitrogen [BUN], and creatinine), and hemorrhage (decreased platelet count). A composite disease characteristic function was introduced to describe disease severity and integrated with the ordinary differential equations estimating the time course of clinical biomarkers. Model simulation results appropriately represented the concentration-dependence of the magnitude and time course of Ebola infection (viral and pathophysiological), including time course of viral load, ALT and AST elevations, platelet count, creatinine, and BUN. The model estimated the observed survival rate in rhesus macaques and the dose of REGN-EB3 required for saturation of the pharmacodynamic effects of viral inhibition, reversal of Ebola pathophysiology, and survival. The model also predicted survival in clinical trials with appropriate scaling to humans. This mathematical investigation demonstrates that drug-disease modeling can be an important translational tool to integrate preclinical data from an NHP model recapitulating disease progression to guide future translation of preclinical data to clinical study design.

[†]Blueprint Medicines, Cambridge, Massachusetts, USA

[‡]Excision BioTherapeutics, New York, New York, USA

This is an open access article under the terms of the [Creative Commons Attribution-NonCommercial-NoDerivs](https://creativecommons.org/licenses/by-nc-nd/4.0/) License, which permits use and distribution in any medium, provided the original work is properly cited, the use is non-commercial and no modifications or adaptations are made.

© 2022 Regeneron Pharmaceuticals. *Clinical and Translational Science* published by Wiley Periodicals LLC on behalf of American Society for Clinical Pharmacology and Therapeutics.

Study Highlights

WHAT IS THE CURRENT KNOWLEDGE ON THE TOPIC?

Ebola virus (EBOV) is recognized as a threat to public health and the burden of an Ebola virus disease (EVD) outbreak cannot be ignored. REGN-EB3 is a combination of three fully human monoclonal antibodies (atoltivimab, maftivimab, and odesivimab-ebgn) that demonstrated reduced fatality rate in patients with EVD when combined with standard of care in the PALM clinical trial.

WHAT QUESTION DID THIS STUDY ADDRESS?

Prior to PALM data availability, a mathematical modeling framework was developed based on preclinical data to describe the antiviral effects and exposure response of REGN-EB3 in non-human primates and to predict survival in humans via translational scaling.

WHAT DOES THIS STUDY ADD TO OUR KNOWLEDGE?

The model predicted survival rates were generally similar with the survival rates observed prospectively in the PALM trial when time to treatment after infection was assumed to be 5 days. Overall, a single, 150 mg/kg dose of REGN-EB3 was seen to offer greatest protection against EBOV. These simulations provide meaningful information regarding the impact of treatment dose as well as time to treatment on the time course of a disease.

HOW MIGHT THIS CHANGE CLINICAL PHARMACOLOGY OR TRANSLATIONAL SCIENCE?

Our model suggests that, with appropriate scaling to humans, drug-disease modeling can be an important translational tool in integrating preclinical data from a relevant animal model to understand disease progression, guide dose selection for future studies and clinical trial design, and predict the probability of survival in preclinical and clinical dose-ranging studies.

INTRODUCTION

Ebola virus disease (EVD) is increasingly recognized as a threat to public health since its emergence in the Democratic Republic of Congo in 1976 and the burden of an Ebola virus (EBOV) epidemic or potential pandemic cannot be ignored.^{1,2} Given the sporadic nature of EBOV outbreaks, conducting randomized controlled trials (RCTs) to enable evaluation of new therapeutics during an outbreak can be difficult.

EBOV, including *Zaire ebolavirus*, one of four known types of the virus from the *Filoviridae* family, is the cause of the severe, often fatal EVD.³ Previously known as hemorrhagic fever, EVD primarily affects humans and other non-human primates (NHPs).³ Initial symptoms of the disease occur within the first week of infection and are nonspecific, including fever, headache, myalgia, vomiting, and diarrhea. Defining symptoms occur in the later stages of disease and can include hemorrhagic manifestations, with internal and external bleeding, multiorgan (kidney and liver) dysfunction and failure, and, in many cases, death (25%–95%).¹ Key hallmarks of EVD are characterized by biomarker-based detection, for example, liver damage in EVD is marked with elevated levels of alanine

(ALT) and aspartate aminotransferases (AST), kidney damage with elevated blood urea nitrogen (BUN), and creatinine and hemorrhage with decreased platelet count. Although several anti-Ebola drugs have been shown to be potent in both animal models² and humans,⁴ the quantitative dynamics of EBOV replication in humans remains unclear, impeding the identification of optimal dose selection or the selection of appropriate combinations of therapeutics.⁵

REGN-EB3 (Inmazeb) is a combination of three human monoclonal antibodies (mAbs), atoltivimab, maftivimab, and odesivimab-ebgn, generated from humanized VelocImmune mice encoding human antibody variable gene segments.² Each of the three mAbs bind distinct, nonoverlapping epitopes on the EBOV glycoprotein and provide complementary mechanisms of action.² In rhesus macaques infected with EBOV, REGN-EB3 administered as either a single- or three-dose regimen in combination from day 5 postinfection demonstrated considerable protection, whereas mortality in control-treated animals was seen uniformly distributed amongst treatment groups by day 9.² Favorable safety, pharmacokinetic (PK) and immunogenicity results from a phase I dose-escalation study in healthy human volunteers

further supported clinical development of REGN-EB3 as a single-dose therapeutic for acute EBOV infection.⁶ In the PALM trial conducted during an EVD outbreak in the DRC, REGN-EB3 plus standard care significantly reduced the usually high fatality rate of EVD compared with ZMapp plus standard care.⁴ In October 2020, REGN-EB3 became the first US Food and Drug Administration (FDA)-approved treatment for EBOV infection in adult and pediatric patients.⁷

It is not always possible to gather dose-ranging data from human challenge studies for infectious diseases with high mortality rates before a medicinal product is approved. As such, animal models which recapitulate EVD characteristics in humans are important for interrogating exposure–response and identifying a dose-regimen that is likely to be safe and efficacious in humans. For Ebola, NHP challenge studies conducted at valid maximum containment Biosafety Level (BSL)-4 laboratory facilities,⁹ provided valuable dose-ranging data, but these studies are difficult to conduct under BSL-4 conditions and as such not every pertinent experimental scenario can be tested.

In these situations, mathematical modeling could provide a relevant link between the available nonclinical data and understanding the experimental treatments available for many human diseases.^{5,9-11} Extrapolation of available information from animal studies to predict outcomes in humans require a framework of dynamic mathematical models and a strong link between models and data such that the model-predicted disease dynamics information can be translated to treatment in humans.^{5,9,11-14} Additionally, biomarkers that are of clinical utility¹⁵ may be used to represent disease progression in modeling.¹⁶⁻¹⁸

A drug-disease model integrating data on viral dynamics, disease pathophysiology, and outcome (e.g., survival), can be complementary to observed preclinical and clinical data, and allows exploration of a hypothesis that can be difficult to test experimentally, especially under BSL-4 conditions where the limited number of infected animals per study become prohibitive to testing multiple hypotheses. Examples of hypotheses that can be explored include the impact of varying time-to-treatment on clinical outcome (e.g., survival) or the effect of various antiviral treatment modalities (e.g., monotherapy vs. combination therapy). The objective of this analysis, which was initiated prior to the availability of data from the PALM RCT, was to develop a computational drug-survival modeling framework to assess and integrate data across different studies and endpoints, and to apply the *in silico* model as a translational tool to predict survival in humans infected with

EBOV and the impact of treatment on survival.^{22,23} Here, we describe the development of a drug-disease model linking the effects of REGN-EB3 neutralization of the EBOV to survival in a rhesus macaque model and subsequent translational scaling to predict survival in humans with treatment.

METHODS

Animal housing

All primates were placed in a BSL-4 laboratory 8 days before virus inoculation where they were fed and cared for daily and allowed to acclimatize to their new surroundings.

Data collection

Drug concentration and pharmacodynamic (PD) data from preclinical single- and multiple-dose studies of REGN-EB3 in infected rhesus macaques, conducted under Institutional Animal Care and Use Committee (IACUC) approval, as described previously,² were used to develop a mathematical modeling framework to predict the drug response in humans and the effect of time to treatment on drug efficacy in infected rhesus macaques. The software platform, MATLAB version 9.4 (R2018A, MathWorks), was used to develop the model and perform all simulations.

Preclinical studies in rhesus macaques infected with the Kikwit Ebola strain were conducted in a blinded manner in a BSL-4 laboratory at the Texas Biomedical Research Institute or the US Army Medical Research Institute of Infectious Diseases. PD data collected from these studies were used to estimate the model parameters.³ Collectively in these studies, 36 animals were inoculated with the EBOV at day 0 and received a single-dose REGN-EB3 treatment on day 5. Data collected included survival rate, and laboratory parameters, such as AST, ALT, BUN, creatinine, and platelet count measured after single dose administration of REGN-EB3 with four doses (10, 50, 100, and 150 mg/kg total dose of the three antibodies combined), with nine animals per dose (Tables 1 and 2). In a separate PK study, 12 rhesus macaques were inoculated at day 0 (originally 14 animals were included but two died, and thus were excluded from the dataset due to insufficient data availability) and treated from day 5 with different doses and regimens of REGN-EB3 as follows: a single dose of 150 mg/kg, two doses of 50 mg/kg 3 days apart, or three doses of 50 mg/kg every 3 days (as shown in Table 1).

TABLE 1 Design aspects of preclinical PD and PK studies in infected rhesus macaques

Property	Value	
Study	PD	PK
BSL-4 facility	USAMRIID	Texas Biomed
Viral route of administration	Intramuscular	Intramuscular
Target inoculation, pfu	1000	1000
Control group, <i>n</i>	4	–
Treated group, <i>n</i>	36	14 ^a
REGN-EB3 dose, mg/kg	Single dose: 10, 50, 100, 150	<ul style="list-style-type: none"> • Single dose: 150 (<i>n</i> = 4) • Multiple dose: 100 (50, days 0 & 3; <i>n</i> = 5) • Multiple dose: 150 (days 0, 3 & 6; <i>n</i> = 3)
Duration, days	35	23
Day of challenge	0	0
Day of first treatment	5	5

Abbreviations: BSL, biosafety level; PD, pharmacodynamic; pfu, plaque-forming units; PK, pharmacokinetic; USAMRIID, US Army Medical Research Institute of Infectious Diseases.

^aTwo animals died due to Ebola infection, and their concentration data were excluded from the model mainly due to sparseness.

TABLE 2 Survival outcomes reported after REGN-EB3 treatment in the preclinical PD study and the PALM trial⁴

Study	REGN-EB3 dose (mg/kg)	No. of animals with EVD at day 0	Survival rate after treatment at day 5
PD study	Control	4	0 (0%)
	10	9	4 (44%)
	50	9	7 (79%)
	100	9	8 (89%)
	150	9	8 (89%)
		No. of patients with EVD at day 1	Survival rate after treatment at day 28
PALM trial	150	155	103 (67%)

Abbreviations: EVD, Ebola virus disease; PD, pharmacodynamic.

Population PK model

Drug concentration data were also collected in this analysis. The drug concentration data were used to develop the population PK model. A two-compartment model with a linear clearance rate was subsequently developed (SimBiology 5.8 toolbox) to estimate the concentration of REGN-EB3 (Figure S1). The parameters associated with the PD biomarkers (e.g., synthesis rate and degradation rate of AST, ALT, BUN, creatinine, and platelet count) were collected and/or estimated using literature data.^{16,18,21-25}

REGN-EB3 serum concentrations in infected rhesus macaque

Serum samples from infected rhesus macaques were analyzed for total REGN-EB3 (all three mAbs combined)

concentrations using an enzyme-linked immunosorbent assay that measured total anti-EBOV human IgG antibodies. The lower limit of quantification was 0.078 µg/ml in neat serum.

Determination of serum viral titers

Analysis of viral load in the sera of infected treated and control animals was conducted by plaque assay, with treatment doses determined on the day of challenge (Table 1; Figure 1a).² On the day before challenge, Vero E6 cells were plated in 6-well plates; serial dilutions of the challenge material were then incubated on the monolayer for 1 h at 37°C. The monolayer was subsequently covered with a 0.5% agarose (SeaKem ME Agarose; Lonza) solution postincubation. Following a 1-week incubation period at 37°C, the cells were then covered with neutral red

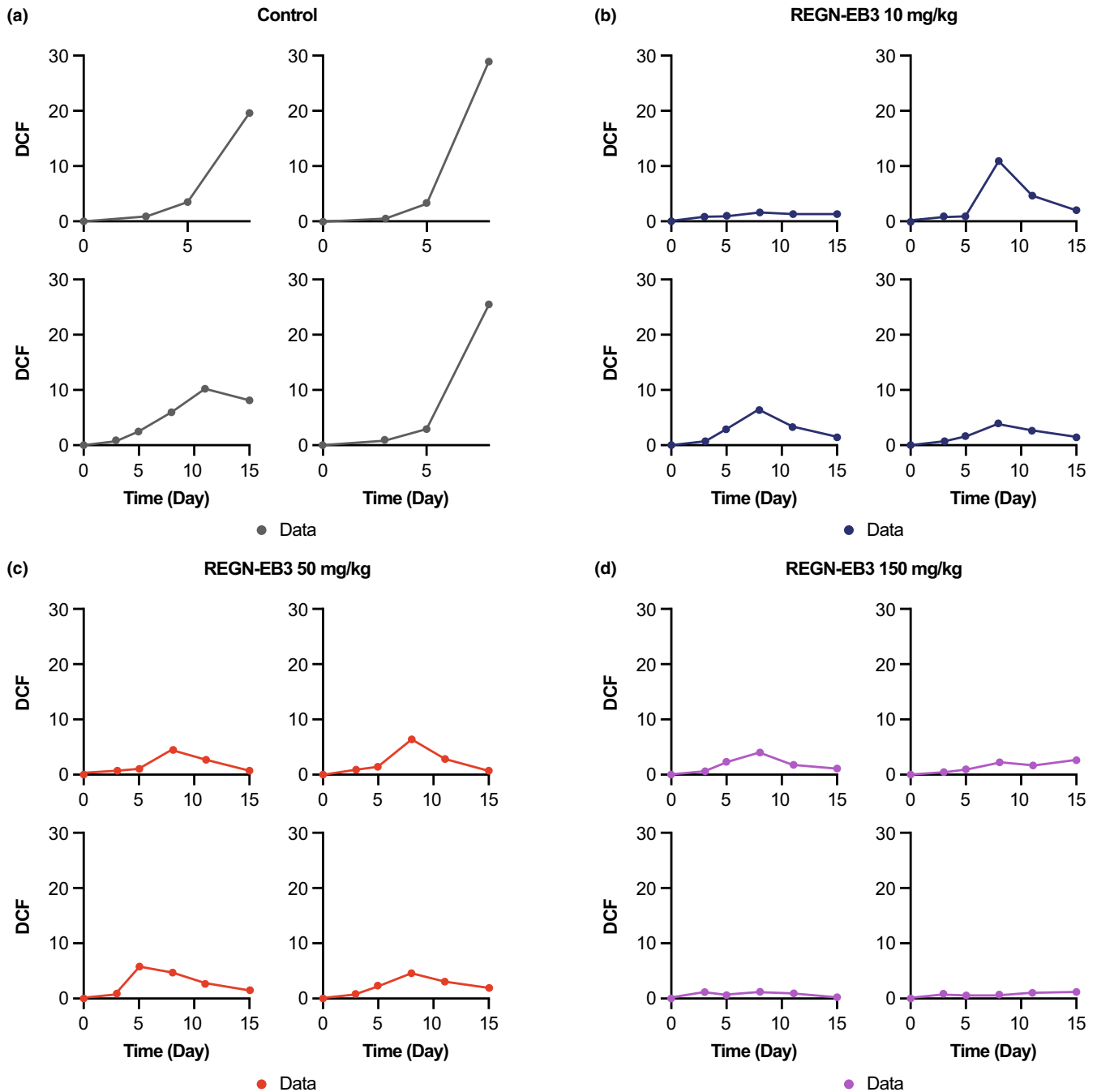


FIGURE 1 Individual time course of disease characteristic function in (a) four euthanized animals in the control group, and (b–d) four animals that survived in the 10, 50, and 150 mg/kg REGN-EB3 groups. All animals were inoculated with EVD on day 0 and received their first treatment on day 5. Scatter plots of DCF were calculated using observed data in the control and four dosing groups (the 100 mg/kg dosing group is not shown here). $DCF(t) = \sum_{i=1}^5 Q_i (x_i(t) - x_{base})$ where $x_i(t)$ and x_{base} were observed biomarker value (i.e., ALT, AST, BUN, PLT, and CR) at time t and baseline, respectively. Q_i was weighting coefficient associated with each hallmark of the disease. The DCF function change over time and behave differently for each group. The function values indicate that the group with higher dose (150 mg) has least disease severity and highest chance of survival. ALT, alanine aminotransferase; AST, aspartate aminotransferase; BUN, blood urea nitrogen; CR, creatinine; EVD, Ebola virus disease; DCF, disease characteristic function; PLT, platelet count.

and were incubated over night at 37°C. The following day, plaques were counted over a light box. This process was repeated to assess animal's viremia, but using serially diluted serum was serially diluted instead of challenge material.

Telemetry and BSL-4 considerations

Telemetry devices were surgically implanted in the rhesus macaques to monitor their temperature throughout these drug concentration and PD studies (T2J; Konigsberg

Instruments). The data were acquired and analyzed digitally using the Notocord-hem Evolution software platform (version 4.3.0.47, Notocord).

Mathematical model development

A viral load-drug dynamics model structure-based on target cell limitation²⁶ (Figure 2a), was developed to assess the viral titer data over time and to the mechanism of action (MOA) of REGN-EB3 in rhesus macaques (Figure S2). To better understand the pharmacology of the drug, the exposure of REGN-EB3 (PK) was linked to important model parameters, such as clearance of infected cells and production rate of virus (δ and p , respectively, from equations 3 and 4 in Supplementary Materials) using a Hill function. In addition to biological plausibility, local sensitivity analysis was conducted to guide selection of these parameters, however, the results are not included in this paper. A semimechanistic modular modeling approach was used to describe the key hallmarks of EVD (i.e., elevated AST, ALT, and BUN, and decreased platelet counts) by connecting each module to viral load dynamics as a driving force for changes in biomarkers (Figure 2b). Using MATLAB version 9.4 (R2018A) as a platform to formulate numerical techniques, a composite disease characteristic function (DCF) was introduced into the model to describe disease severity and integrated with the ordinary differential equations (presented in Supplementary Materials) estimating the time course for all clinical biomarkers, as depicted in Figure 2c. Scatter plots of DCF were calculated using the equation $DCF(t) = \sum_{i=1}^5 Q_i (x_i(t) - x_{i,base})$ where $x_i(t)$ and $x_{i,base}$ are observed biomarker values (i.e., ALT,

AST, BUN, PLT, and CR) at time t and baseline, respectively. Q_i is weighting coefficient associated with each hallmark of the disease (Supplementary Methods). The time-varying DCF score was converted to probability of survival using the Kaplan–Meier (KM) estimator to assess the probability of survival (this method is often used to measure the fraction of patients' lifespan for a certain amount of time after treatment)²⁷ and the Monte Carlo Simulation sampling method. The REGN-EB3 survival model structure describes the MOA of REGN-EB3 and the pathophysiology of EVD (Figure S2). To describe the concentration–time profile of REGN-EB3 in infected rhesus macaques' serum, a two-compartment population PK model with linear clearance was developed (SimBiology 5.8 toolbox) and used to fit the PK data from the infected rhesus macaque from the NHP PK study. The model structure along with its differential equations are presented in Supplementary Materials.

Model scaling to humans

The rules applied to translate PK/PD parameters between rhesus macaque monkeys and humans included use of the equation: $Y = p \cdot BW^b$, where Y is the parameter of interest, p the weight independent parameter, and BW is body weight.²⁸ Typically, b is assumed to be $-1/4$ for first order rate constants and $3/4$ for zero order constants. Drug-related parameters were not transformed, and amplification factor, interindividual variability, residual error, and dimensionless parameters were not scaled. The average metabolic rate of a cell is lower in larger species and the metabolic rate affects the rate at which a cell synthesizes

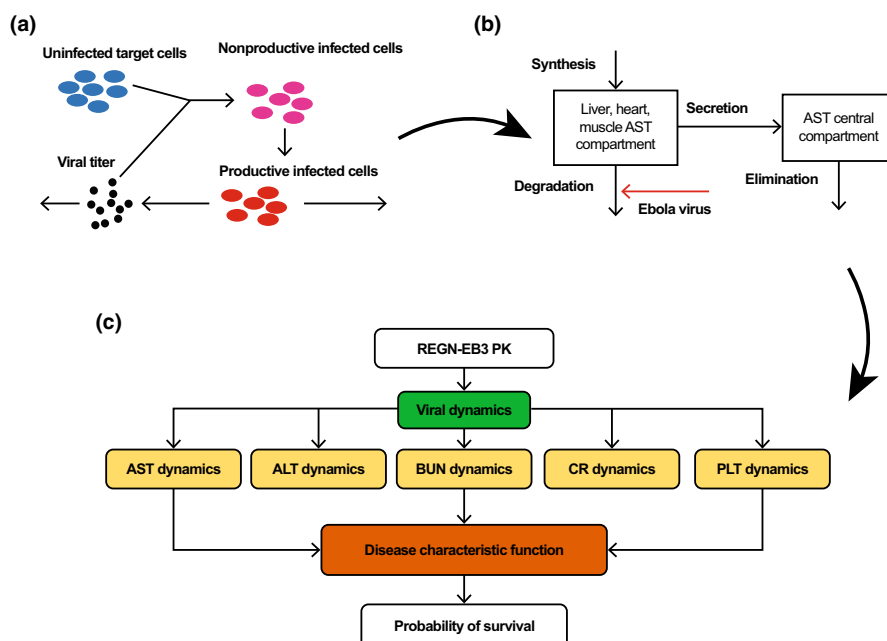


FIGURE 2 REGN-EB3 survival model structure developed from (a) a viral load dynamic model structure; (b) a semimechanistic model structure describing the dynamics of AST (as an example for illustration purposes) in the presence of EBOV; and (c) REGN-EB3 mechanism of action and the disease pathophysiology of Ebola. ALT, alanine aminotransferase; AST, aspartate aminotransferase; BUN, blood urea nitrogen; CR, creatinine; EBOV, Ebola virus; PK, pharmacokinetic; PLT, platelet count.

deoxyribonucleic acid and proteins, and therefore could affect virus replication; viral replication and T-cell proliferation are slower in larger species. The circulation of T-cells through blood, tissues, and the lymphatic system, which function to eliminate the virus, has been suggested to underlie the generating scaling law.²⁹ Biological parameter values (Table 3) are used for predictability scaling to humans from the literature (in vivo studies) rather than the use of an allometric scaling approach.

A similar immune system response was assumed for both human and NHP,³⁰ and the same values for rates of virus production and infected cell removal were used in the viral load dynamics model. The virus clearance rate was scaled using a general scaling law with the power of $-1/4$. Biological parameters in the model were adjusted using data from the literature. From the literature, we learned that clinical end point values in patients infected with EBOV have the same trend as that seen in rhesus macaque models.³¹ The peak values for AST, ALT, creatinine, and BUN in fatal cases were generally consistent with those found in infected rhesus macaque models. Therefore, the current DCF has been used as a criterion for survival analysis, which includes AST, ALT, creatinine, BUN, and platelet counts, with different peak values for BUN and creatinine.

Model validation using clinical trial data

Prior to performing this analysis, a single i.v. dose of REGN-EB3 150 mg/kg was selected for evaluation from the Expanded Access Protocol and the PALM RCT.⁴ The population PK model developed in infected rhesus macaques was allometrically scaled to humans to estimate exposure to REGN-EB3 in infected humans at the dose of 150 mg/kg to understand how exposure for this dose in infected humans compared to those associated with maximal efficacy in infected rhesus macaques. To compare predicted survival rates using a scaled model and results from the PALM trial, two simulation scenarios were performed where time of treatment after infection was varied. In the first scenario, 500 virtual patients were created and exposed to REGN-EB3 150 mg/kg at day 5 of infection. For the second simulation, the same virtual population was treated after 2–5 days of infection.

RESULTS

Model predictability by viral load

An overlay of model performance and viral load—time profiles of animals treated with a single dose of REGN-EB3

(10, 50, 100, or 150 mg/kg) demonstrated that the developed model effectively describes the therapeutic effect of REGN-EB3 on EVD. As depicted in Figure 3a, viral load in serum peaked at day 5 after infection, which was also when treatment with REGN-EB3 started. The viral load decreased rapidly with higher doses of REGN-EB3 (100 or 150 mg/kg, single dose) compared with lower doses (10 or 50 mg/kg, single dose). In addition to viral load, the model was able to capture the observed disease pathophysiology data, including AST, ALT, and platelet count levels, as shown in Figures 3b–d, and BUN and creatinine levels, as shown in Figures S3A,B. Figures S1A,B summarizes the performance of the population PK model developed through the comparison of model-predicted and observed concentration values of REGN-EB3.

Effect of REGN-EB3 on disease characteristic function

The DCF contains a composite function of disease pathophysiology information at a specific time. The individual effect–time profiles of DCF, which depicts EVD progression, are shown for different groups of animals in Figure 1. The function over time indicates the time course of disease severity in control and treated groups. As shown in Figure 1a, the untreated group (control) had the highest disease scores over time when compared with the treated groups. As the treatment started on day 5, the DCF values calculated based on observed data decreased over time for the treated groups (REGN-EB3 doses 10, 50, and 150 mg/kg; Figures 1b–d). From day 5 to day 15, the highest dose of REGN-EB3 (150 mg/kg) led to a steady decrease in DCF values and did not deviate significantly from the baseline values before inoculation compared with the other groups (Figure 1d). As the DCF value increased, the probability of survival decreased, as seen in the control group (Figure 1a).

Predicted survival in rhesus macaques treated with REGN-EB3

To evaluate the performance of our model in predicting survival rates in animal studies, virtual animals were created using an MCS sampling method. Two hundred virtually sampled rhesus macaques were treated with a single i.v. dose of REGN-EB3 at different doses on day 5. Comparison of observed survival rates from the PD study, 44%, 79%, 89%, and 89% for doses of 10, 50, 100, and 150 mg/kg, respectively, together with the simulation results, demonstrated the capability of the developed model to predict the survival rate for different dosing regimens as

TABLE 3 Drug-disease model parameters

Property	Value from rhesus macaque model	Value from human model	Reference	Assumption
ALT and AST degradation in rat cell, 1/day	3	–	Literature	Same for monkey
AST half-life in human serum, hours	17 ± 5	–	Literature	Used allometric for monkey
ALT half-life in human serum, hours	47 ± 10	–	Literature	Used allometric for monkey
Liver AST and ALT activity in liver compared with blood	~10	–	Literature	Used to estimate liver AST and ALT concentration
Human serum AST, U/L	10–40	–	Literature	–
Monkey serum ALT, U/L	27 ± 6	–	In-house data	–
Monkey serum AST, U/L	29 ± 6	–	In-house data	–
Delay in viral action on liver function, days	~2–3	–	In-house data	–
Platelet lifespan for mammals, days	5–10	–	Literature	–
Normal platelet counts for humans, per μl	–	150,000–450,000	Literature	–
Normal platelet counts for monkeys, per μl	328,000	–	In-house data	–
CR volume of distribution (human), L	–	33–41	Literature	Used allometric for monkeys
CR clearance rate (human), ml/min	–	35	Literature	Used allometric for monkeys
Normal BUN for human, mg/dl	–	7–20	Literature	–
Normal BUN for monkey, mg/dl	14.5	–	In-house data	–
λ , cell/day	5×10^5 (fixed)	5×10^5	–	–
μ , 1/day	0.001 (fixed)	0.001	–	–
β , 1/day* \log_{10} (GE/ml)	0.2045 (fixed)	0.2045	–	–
τ , day	2 (fixed)	2	–	–
δ , 1/day	2.73 (estimated)	2.73	–	–
P, 1/day	0.001 (estimated)	0.001	–	–
γ , 1/day	0.17 (estimated)	0.17	Estimated	–
Population PK parameter estimates of total anti-EBOV human IgG antibodies in infected rhesus macaque monkeys				
CL (ω), ml/kg/day	8.4 (0.13)	–	Estimated	–
V1 (ω), ml/kg	47.88 (0.13)	–	Estimated	–
V2 (ω), ml/kg	52.1 (2.2)	–	Estimated	–
Q (ω), ml/kg/day	23.74 (0.0062)	–	Estimated	–
DCF parameter values associated with each biomarker				
Q_ALT	8	–	Estimated	–
Q_AST	5	–	Estimated	–
Q_BUN	10	–	Estimated	–
Q_PLT	3	–	Estimated	–
Q_CR	9	–	Estimated	–
Hill function parameter in viral load dynamics				
Vm1, 1/day	3.5	–	Estimated	–
Km1	5.2	–	Estimated	–
N1	5	–	Estimated	–

(Continues)

TABLE 3 (Continued)

Property	Value from rhesus macaque model	Value from human model	Reference	Assumption
Vm2, 1/day	3.4	–	Estimated	–
Km2	4.8	–	Estimated	–
N2	3	–	Estimated	–
Vm3, 1/day	1.3	–	Estimated	–
Km3	3.05	–	Estimated	–
N3	1.35	–	Estimated	–
Vm4, 1/day	2.3	–	Estimated	–
Km4	9.7	–	Estimated	–
N4	0.78	–	Estimated	–
Vm5, 1/day	3.08	–	Estimated	–
Km5	9.9	–	Estimated	–
N5	9	–	Estimated	–
Vm6, 1/day	2.7	–	Estimated	–
Km6	13	–	Estimated	–
N6	1.2	–	Estimated	–

Abbreviations: ω , random effect; ALT, alanine aminotransferase; AST, aspartate aminotransferase; BUN, blood urea nitrogen; CR, creatinine; CL, clearance; DCF, disease characteristic function; EBOV, Ebola virus; Km, Hill constant; N, Hill coefficient; PK, pharmacokinetic; PLT, platelet count; Q, intercompartmental clearance; V1, volume of distribution of central compartment; V2, volume of distribution of peripheral compartment; Vm, maximum rate constant.

illustrated in simulated KM curves (Figure 4a). The model adequately estimated the observed survival rate in rhesus macaques and all REGN-EB doses that resulted in saturation of the PD effects of viral inhibition, reversal of Ebola pathophysiology, and survival.

Predicted survival in humans infected with EBOV

To evaluate the predictability of our model translated from NHPs to humans, we created 500 virtual patients using the scaled model. Comparison of survival rate from the simulation for an REGN-EB3 dose of 150 mg/kg (70%) and observed data in the PALM RCT (67%) shows that the model prediction of survival was consistent with acceptable accuracy (Figure 4b).⁴ Concordance with the actual data was dependent on the time to treatment in the simulation scenario. As shown in Figure 4b, the scenario where treatment was started 5 days after infection in the simulated model showed the greatest concordance with the observed data (70% vs. 67%, respectively), whereas starting treatment 2–5 days after symptom onset in the simulated model resulted in higher predicted survival compared with the observed data from the PALM trial (82% vs. 67%, respectively).

DISCUSSION

This paper describes the development of an integrated model linking EBOV load and relevant disease pathophysiology (including changes in disease characteristic biomarkers, such as ALT, AST, creatinine, and BUN) to predict the outcome of survival in a rhesus macaque infection model. This modeling approach can be used in conjunction with preclinical data, to support antiviral drug development when conducting dose ranging using a human-challenge study is not feasible (e.g., BSL-4 conditions or when a patient population is not accessible). Using this model, we were able to successfully predict survival in NHPs and, with appropriate scaling, to predict survival in humans comparable to that observed in a human clinical trial (PALM trial), with treatment.⁴ Although our model was developed based on preclinical NHP data, the ability of the model to predict survival in the clinical setting is significant due to the practical challenges associated with designing a prospective RCT in EVD.

The model was able to capture the dynamics of disease pathophysiology in the presence of treatment. The simulations indicated that higher doses (both 100 and 150 mg/kg) of REGN-EB3 in the animal study resulted in the disease biomarkers returning to baseline levels more rapidly, thereby increasing the probability of survival.

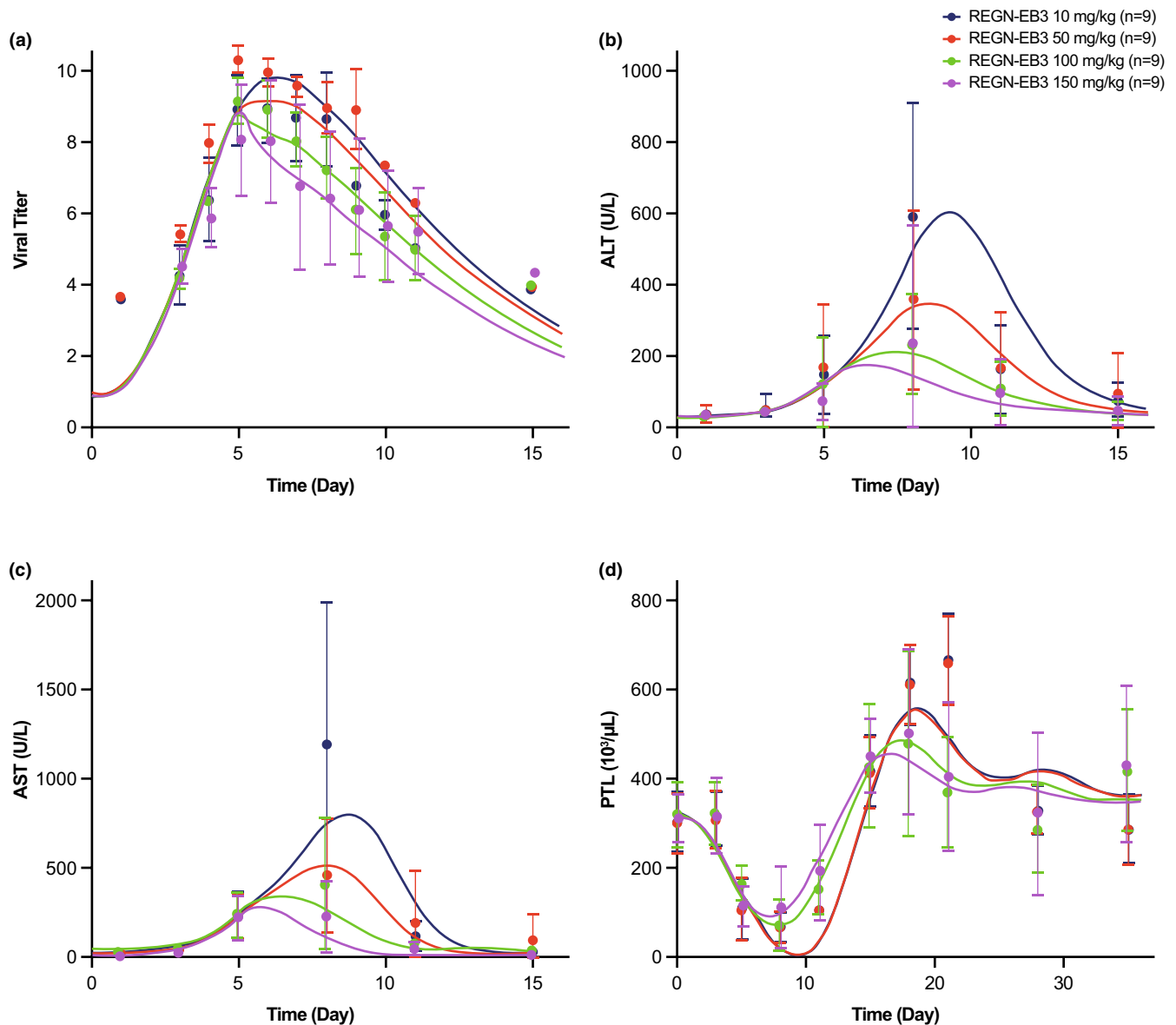


FIGURE 3 Model performance versus mean observed data (\pm SD) in each dose group for hallmarks of EVD following inoculation of animals with EBOV on day 0 and treatment with a single dose of REGN-EB3 on day 5, including (a) viral titer, and time course of (b) ALT, (c) AST, and (d) platelet. The dots (\bullet) represent mean observed survival data and lines (—) are the model predictions (simulated profiles). The model captures the dynamics of observed viral titer and biomarker data. Viral load was collected at different times. From one dataset, viral load was collected at d1, d3, d5, d8, d11, d14, d21, and d28, and for another study was collected at d1, d2, d3, d3, d4, d5, d6, d7, d8, d9, d10, d11, d12, d18, d21, d28, and d35. It shows that a higher dose of REGN-EB3 (150 mg/kg) was more effective at reducing viral load, returning biomarkers to baseline levels, and enhancing the chance of survival. ALT, alanine aminotransferase; AST, aspartate aminotransferase; d, day; EBOV, Ebola virus; EVD, Ebola virus disease; PLT, platelet count.

The simulated survival data were generally similar with the actual observed data in the rhesus macaque model. Because the actual viral time course in comparison to controls could not be determined due to the four deaths in the control group, these simulations provided meaningful information regarding the impact of treatment on the time course of the disease.

Concordance of model predictions of human survival was dependent on time to treatment initiation relative to

EBOV infection. When the time to treatment was assumed to be 5 days after infection with an i.v. dose of REGN-EB3 150 mg/kg, the predicted survival rate was 70% compared with 66.5% observed in the PALM trial. However, concordance with the observed PALM data was less when the time to treatment was assumed to be 2–5 days after infection, where the predicted survival rate was 82%. These results suggest that earlier administration of REGN-EB3 would have resulted in a higher survival rate. The time to

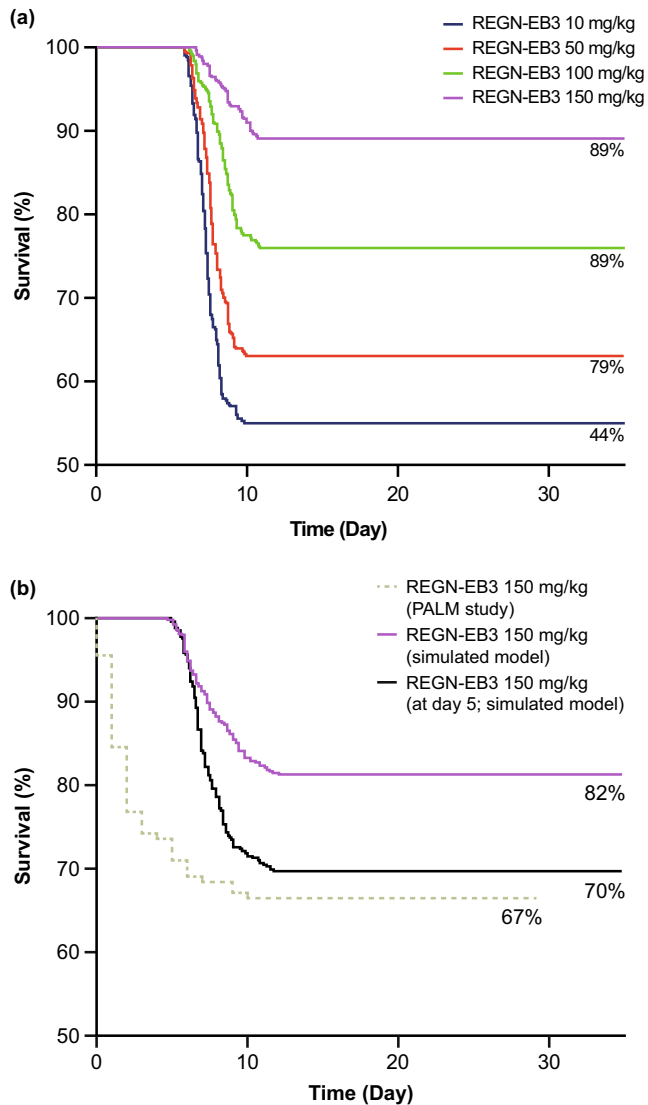


FIGURE 4 (a) Simulated KM curves for REGN-EB3-treated animals (solid lines) showing actual observed survival rate (% provided below each line) and (b) simulated model survival curve for REGN-EB3-treated humans and actual observed curve from REGN-EB3-treated humans in the PALM trial⁶ showing steady state survival rates. (a) The simulated KM curves show adequate consistency between observed and estimated survival rates in infected animal studies. (b) The comparison of simulated survival rate in a clinical setting and observed survival rate in the PALM study (green dotted line) indicates the predictability power of the model. In the simulation (purple line), it was assumed that 500 virtual patients received treatment after 2–5 days of infection. The survival rate related to these patients receiving the treatment at day 5 after infection is shown in a black line. The simulation results obtained using a scaled model were generally similar with the observed data. In addition, it indicates that treatment can increase the chances of survival when provided early. KM, Kaplan–Meier.

treatment effect described by our model is consistent with the pharmacology of one of the antibodies of REGN-EB3, which acts to neutralize Ebola EBOV glycoprotein, inhibiting viral entry into the host cells.

The ability of the model to predict survival while altering certain variables, such as time to treatment relative to infection, is important given that whereas the PALM trial was a prospective, multicenter, multi-outbreak, randomized, controlled safety and efficacy trial,⁵ generation of future RCT data may be difficult due to the extreme circumstances experienced during an epidemic or a pandemic. Reliance on *in silico* methods to address unanswered questions can be extremely valuable, especially when used in conjunction with animal models to predict survival in humans.

This integrated model has several strengths; first, it can be used to understand the dose response based on differing time to treatment relative to infection as illustrated, and, second, to predict the effectiveness of antiviral therapies (acting on different parts of the viral life cycle) when used in combination. These advantages are especially important when multiple scenarios cannot be tested experimentally (e.g., BSL-4 conditions). This model can also be used in developing other EVD antiviral therapies, which have different mechanisms of action, by testing different hypotheses.

There are also several limitations to these analyses. It may not be possible to fully capture the disease spectrum (e.g., this model did not account for fever/temperature or other biomarkers of the disease progression, such as white blood cell count). Factors that may potentially affect the PKs of REGN-EB3, such as baseline viral titers and baseline soluble glycoproteins levels, were not evaluated in this model. The PK model was developed using semi-sparse PK data from a small number of animals ($n = 12$). PD data were also limited; the model only used data from the treated groups to fully characterize the disease, there were challenges acquiring samples from rhesus macaques due to BSL-4 regulations, and full characterization of the natural history of EBOV infection (without treatment) was not possible due to the limited data set (four animals in the control group). The limited number of animals in each treatment group also made it difficult to describe uncertainty around the survival estimates using the model. Another challenge was the lack of human serum levels from REGN-EB3 treated patients due to inability to transport EBOV blood samples for testing. The model did not evaluate the effect of a wide range of patient characteristics, such as sex, ethnicity, and BW, on exposures to the individual mAbs of REGN-EB3 through population PK based simulations. The actual time from infection to treatment in humans is unknown and therefore extrapolation of data from a rhesus macaque model to a human is limited and should be interpreted with caution. Interindividual variability of drug-related parameters was not scaled in this model; however, existing literature reports interindividual

variation in humans for the parameters of the biomarkers used in this model.³²⁻³⁴

In the future, effective treatments will be urgently needed to avoid a crisis in the event of a novel infectious viral disease. Mathematical analysis of viral replication dynamics and treatment strategies in a challenge animal model, such as rhesus macaques, which recapitulates aspects of viral disease progression in humans, has increased our understanding of disease mechanisms, and may aid in the development of novel therapeutics (alone or in combination), prediction of survival and disease management, including healthcare resourcing.²⁹

In conclusion, with a clinically relevant animal model of disease, and knowledge of meaningful PD markers and appropriate scaling to humans, drug-disease modeling can be an important translational tool to predict the probability of survival in preclinical dose-ranging studies as well as in clinical trials. Our model proposes a new pathway for integration of data across different studies and end points, and could be used to predict the probability of survival in preclinical dose-ranging studies and to guide dose selection for future investigations where generating RCT data in humans may be challenging. The scaled model can also be used to look at the impact of patient baseline viral load and minimum dose required to rapidly decrease viral load.

AUTHOR CONTRIBUTIONS

M.K.T. wrote the manuscript. All authors designed and performed the research and analyzed the data.

ACKNOWLEDGMENTS

The authors thank the US Army Medical Research Institute of Infectious Diseases for conducting animal studies and the Biomedical Advanced Research and Development Authority for funding the animal studies. Medical writing support, under the direction of the authors, was provided by Rhutika Dessai, MSc, of Core, London, UK, funded by Regeneron Pharmaceuticals, according to good publication practice guidelines ([link](#)). The sponsor was involved in the study design and collection, analysis, and interpretation of data, as well as data checking of information provided in the paper. The authors were responsible for all content and editorial decisions, and received no honoraria related to the development of this publication.

FUNDING INFORMATION

This study was funded by Regeneron Pharmaceuticals.

CONFLICT OF INTEREST

M.K.T., N.H., J.D.D., A.B., C.A.K., J.K., A.T.DiC., and M.A.K. are Regeneron Pharmaceuticals, Inc. employees/stockholders. C.K. has issued patents (U.S. Patent Nos.

10,787,501, 10,954,289, and 10,975,139) and pending patents, which have been licensed and receiving royalties, with Regeneron Pharmaceuticals, Inc. S.S. is an Excision BioTherapeutics employee/stockholder and former Regeneron Pharmaceuticals, Inc. employee and current stockholder. R.R. is an employee of Blueprint Medicines and former Regeneron Pharmaceuticals, Inc. employee.

ORCID

John D. Davis  <https://orcid.org/0000-0001-6282-1670>

REFERENCES

1. Van Kerkhove MD, Bento AI, Mills HL, Ferguson NM, Donnelly CA. A review of epidemiological parameters from Ebola outbreaks to inform early public health decision-making. *Sci Data*. 2015;2:150019.
2. Pascal KE, Dudgeon D, Trefry JC, et al. Development of clinical-stage human monoclonal antibodies that treat advanced Ebola virus disease in nonhuman primates. *J Infect Dis*. 2018;218:S612-S626.
3. World Health Organization. Ebola virus disease. 2021. https://www.who.int/health-topics/ebola#tab=tab_1. 11 January 2022.
4. Mulangu S, Dodd LE, Davey RT Jr, et al. A randomized, controlled trial of Ebola virus disease therapeutics. *N Engl J Med Overseas*. 2019;381:2293-2303.
5. Martyushev A, Nakaoka S, Sato K, Noda T, Iwami S. Modelling Ebola virus dynamics: Implications for therapy. *Antiviral Res*. 2016;135:62-73.
6. Sivapalasingam S, Kamal M, Slim R, et al. Safety, pharmacokinetics, and immunogenicity of a co-formulated cocktail of three human monoclonal antibodies targeting Ebola virus glycoprotein in healthy adults: a randomised, first-in-human phase 1 study. *Lancet Infect Dis*. 2018;18:884-893.
7. US Food & Drugs Administration. FDA approves first treatment for ebola virus [media release]. 14 Oct 2020. <https://www.fda.gov/news-events/press-announcements/fda-approves-first-treatment-ebola-virus>
8. Piorkowski G, Jacquot F, Quérat G, et al. Implementation of a non-human primate model of Ebola disease: Infection of Mauritian cynomolgus macaques and analysis of virus populations. *Antiviral Res*. 2017;140:95-105.
9. Keeling MJ, Danon L. Mathematical modelling of infectious diseases. *Br Med Bull*. 2009;92:33-42.
10. Khaksar Toroghi M, Bosley J, Powell LM, et al. A quantitative systems pharmacology modeling platform for evaluating triglyceride profiles in patients with high triglycerides receiving evinacumab. *CPT Pharmacometrics Syst Pharmacol*. 2021;10:1332-1342.
11. Chretien JP, Riley S, George DB. Mathematical modeling of the West Africa Ebola epidemic. *eLife*. 2015;4:e09186.
12. Wong ZS, Bui CM, Chughtai AA, Macintyre CR. A systematic review of early modelling studies of Ebola virus disease in West Africa. *Epidemiol Infect*. 2017;145:1069-1094.
13. Agosto FB. Mathematical model of Ebola transmission dynamics with relapse and reinfection. *Math Biosci*. 2017;283:48-59.
14. Jiang S, Wang K, Li C, et al. Mathematical models for devising the optimal Ebola virus disease eradication. *J Transl Med*. 2017;15:124.

15. Bergman KL. The animal rule: the role of clinical pharmacology in determining an effective dose in humans. *Clin Pharmacol Ther.* 2015;98:365-368.
16. Kim WR, Flamm SL, Di Bisceglie AM, Bodenheimer HC. Public Policy Committee of the American Association for the Study of Liver, D. Serum activity of alanine aminotransferase (ALT) as an indicator of health and disease. *Hepatology.* 2008;47:1363-1370.
17. Rollin PE, Bausch DG, Sanchez A. Blood chemistry measurements and D-Dimer levels associated with fatal and nonfatal outcomes in humans infected with Sudan Ebola virus. *J Infect Dis.* 2007;196(Suppl 2):S364-S371.
18. Lee KL, Darke PL, Kenney FT. Role of coenzyme in aminotransferase turnover. *J Biol Chem.* 1977;252:4958-4961.
19. Toroghi M, Davis J, DiCioccio A, et al. A novel integrated viral dynamics disease model predicting survival in ebola infection. *Clin Pharmacol Ther.* 2020;107(Suppl. 1):S5-S121.
20. Toroghi M, Kamal M, Kantrowitz J, DiCioccio T, Rippley R. A novel pathophysiological drug-survival mathematical modeling framework for Ebola virus disease. 10th American Conference on Pharmacometrics ACoP10. 2019.
21. Chimela W, Mesua N, Abdulraheem B-A. Aspartate Transaminase (AST) activity in selected tissues & organs of clarias gariepinus exposed to different levels of paraquat. *J Environ Anal Toxicol.* 2014;4:214.
22. O'Sullivan ED, Doyle A. The clinical utility of kinetic glomerular filtration rate. *Clin Kidney J.* 2017;10:202-208.
23. Ballem PJ, Belzberg A, Devine DV, et al. Kinetic studies of the mechanism of thrombocytopenia in patients with human immunodeficiency virus infection. *N Engl J Med.* 1992;327:1779-1784.
24. Milo R, Jorgensen P, Moran U, Weber G, Springer M. BioNumbers—the database of key numbers in molecular and cell biology. *Nucleic Acids Res.* 2010;38:D750-D753.
25. Wishart DS, Feunang YD, Marcu A, et al. HMDB 4.0: the human metabolome database for 2018. *Nucleic Acids Res.* 2018;46:D608-D617.
26. Zitzmann C, Kaderali L. Mathematical analysis of viral replication dynamics and antiviral treatment strategies: from basic models to age-based multi-scale modeling. *Front Microbiol.* 2018;9:1546.
27. Dinse GE, Lagakos SW. Nonparametric estimation of lifetime and disease onset distributions from incomplete observations. *Biometrics.* 1982;38:921-932.
28. Zuideveld KP, Van der Graaf PH, Peletier LA, Danhof M. Allometric scaling of pharmacodynamic responses: application to 5-Ht1A receptor mediated responses from rat to man. *Pharm Res.* 2007;24:2031-2039.
29. Althaus CL. Of mice, macaques and men: scaling of virus dynamics and immune responses. *Front Microbiol.* 2015;6:355.
30. Haigwood NL, Walker CM. *Commissioned Paper: Comparison of Immunity to Pathogens in Humans, Chimpanzees, and Macaques.* National Academies Press; 2011.
31. Vernet MA, Reynard S, Fizet A, et al. Clinical, virological, and biological parameters associated with outcomes of Ebola virus infection in Macenta, Guinea. *JCI Insight.* 2017;2:e88864.
32. Carobene A, Braga F, Roraas T, Sandberg S, Bartlett WA. A systematic review of data on biological variation for alanine aminotransferase, aspartate aminotransferase and gamma-glutamyl transferase. *Clin Chem Lab Med.* 2013;51:1997-2007.
33. de Gaetano G, Santimone I, Gianfagna F, Iacoviello L, Cerletti C. Variability of platelet indices and function: acquired and genetic factors. *Handb Exp Pharmacol.* 2012;210:395-434.
34. Naresh CN, Hayen A, Weening A, Craig JC, Chadban SJ. Day-to-day variability in spot urine albumin-creatinine ratio. *Am J Kidney Dis.* 2013;62:1095-1101.

SUPPORTING INFORMATION

Additional supporting information can be found online in the Supporting Information section at the end of this article.

How to cite this article: Toroghi MK, Al-Huniti N, Davis JD, et al. A drug-disease model for predicting survival in an Ebola outbreak. *Clin Transl Sci.* 2022;15:2538-2550. doi:[10.1111/cts.13383](https://doi.org/10.1111/cts.13383)